Assessment of *σ*-Diatropicity of the Cyclopropane Molecule

Stefano Pelloni,[†] Paolo Lazzeretti,*,[†] and Riccardo Zanasi[‡]

Dipartimento di Chimica dell'Università degli Studi di Modena e Reggio Emilia, Via Campi 183, 41100 Modena, Italy, and Dipartimento di Chimica dell'Università degli Studi di Salerno, via Ponte don Melillo, 84084 Fisciano (SA), Italy

Spatial models of the current density field induced in the cyclopropane molecule by stationary, homogeneous magnetic fields, parallel to either the C_3 or the C_2 symmetry axis, have been constructed. A compact, abridged representation of the models is given via stagnation graphs that convey essential information. Maps of streamlines and moduli are also reported to complete current models that have proven useful to rationalize magnetic tensor properties, that is, magnetizability, ^{1}H and ^{13}C nuclear shieldings, and magnetic shielding along the C_3 symmetry axis. Plots of Biot−Savart magnetic shielding density combined with current density visualization yield an accurate, detailed account of the shielding mechanisms. The magnetropicity of the system described by the current density model is fully consistent with the magnitude of magnetic tensors calculated at near Hartree−Fock level. In a field perpendicular to the molecular plane, cyclopropane sustains a diatropic $σ$-ring current with the following peculiar features: (i) it follows the molecular periphery rather than the CC framework; (ii) it bifurcates in the proximity of the methylene moieties flowing along the CH bonds, both above and below the $σ_h$ plane; (iii) it has an effect on the values of response properties, although it is not as large as expected from naive arguments (e.g., the center-of-mass value of the magnetic shielding constant is dominated by in-plane components rather than the out-of-plane component, which is in contrast to $π$-aromatic systems such as benzene); (iv) it has a negligible effect on the strong anisotropy of carbon magnetic shielding, which is shown to arise from local currents. No evidence for strong diatropism, and therefore $σ$-aromaticity of the cyclopropane molecule, was found on the magnetic criterion.

1. Introduction

The smallest cyclic molecule formed by three CH_2 units (cyclopropane) is characterized by a peculiar electronic structure, described in qualitative terms by the Walsh model[1−3] or equivalently by bent bond orbitals à la Coulson and Moffitt.[4,5] The theory predicts some amount of $σ$-electron delocalization related to resonance and to strained geometry.[2,5] As a consequence, C_3H_6 possesses unusual energetic[6−9] and spectroscopical[10−14] properties that have been the object of much investigation. Chemists traditionally assumed that cyclopropane is endowed with a special combination of qualities that is referred to as $σ$-aromaticity.[15−17] Dewar pointed out that benzene and cyclopropane are isoconjugated, as both molecules are stabilized by a sextet of strongly delocalized electrons. Whereas the former is $π$-aromatic, the latter is $σ$-aromatic.[6] Moran et al. even refer to C_3H_6 as the archetypal $σ$-aromatic system.[18]

Pascal was the first to underline the typical magnetic properties of this molecule.[19,20] The experimental average susceptibility[21,22] of C_3H_6 is considerably bigger than that obtained from additive schemes,[23] and its anomalous anisotropy, more recently measured with increasing accuracy,[13,14] was attributed by Wiberg and Nist[10] to the presence of $σ$-ring currents induced by a magnetic field perpendicular to the molecular plane, which also causes upfield ^{1}H nuclear magnetic resonance (NMR) chemical shift.

The concept of $σ$-ring currents has been accepted by many authors.[11,24−27] Jao et al. reported a magnetic exaltation as big as one-third that of benzene,[28] which is thought to arise from the precession of mobile $σ$-conjugated electrons. Long range ^{1}H shielding attributed to cyclopropane ring currents was advocated to assign molecular configurations.[24,29,30] Abnormally high calculated values of nucleus independent chemical shift (NICS)[31] are considered to be consistent with $σ$-diatropicity.[9,18,27,30]

According to a model developed by Dewar, see Figure 4a of ref 6 on $σ$-conjugation, the upfield proton resonance shift can be understood in terms of an aromatic ring current in the cyclopropane ring, supposing that the hydrogen nuclei lie in the shielded region of the anisotropy cone. However, a ring current model does not explain the anomalous isotropic upfield chemical shift (≈20 ppm) of the ^{13}C of methylenes reported by Zilm et al.[12] Nor does it justify the strong anisotropy of the experimental carbon chemical shift, which is due to only one component ($δ_{33}^C$), whereas the other two components of the shift tensor ($δ_{11}^C$ and $δ_{22}^C$) have typical aliphatic values, according to Zilm et al.[12]

It is commonly accepted that the local effect on a benzenic C nucleus, determined by the diamagnetic ring currents in which it is immersed, vanishes as the induced Biot−Savart magnetic field changes sign on crossing the current stream.[32] However, there is theoretical evidence for a sizable contribution (≈10%) of $π$-ring currents to carbon shielding in benzene, arising from electron circulation about remote carbon nuclei, as shown by magnetic shielding density maps.[33−35] At any rate,

* To whom correspondence should be addressed. E-mail: lazzeret@unimo.it.
† Università degli Studi di Modena e Reggio Emilia.
‡ Università degli Studi di Salerno.

a similar mechanism is not expected to be responsible for the surprising high-field value of δ^{C}_{33} in benzene and cyclopropane.

A model for the current density induced by a stationary magnetic field perpendicular to the ring plane, according to which C_3H_6 does not sustain London-type ring currents, was reported in 1983.[36] However, the reliability of this model is questionable, as it is affected by at least three unsatisfactory features. (1) It is not invariant to a change of coordinate frame, because it was obtained within the coupled Hartree−Fock (CHF) approximation, which allows for the common origin (CO) approach that is now superseded by translationally invariant methods based on continuous transformation of the origin of the current density (CTOCD),[37−42] formally annihilating either the diamagnetic or paramagnetic contributions to the quantum mechanical current density, that is, diamagnetic-zero (DZ) or paramagnetic-zero (PZ), and by methods employing gauge-including atomic orbital (GIAO) basis sets.[43,44] (2) It does not accurately represent the electron circulation about the carbon nuclei, which does not allow inference on the origin of the abnormally high σ^{C}_{33}. (3) It yields insufficient information on current density in space.

Therefore, an improved model is needed to provide a realistic description of the current density induced by an external magnetic field. Such a model is required to rationalize the magnitude of in-plane and out-of-plane components, the average value of tensor properties that are experimentally available, that is, magnetizability and chemical shifts of hydrogen and carbon nuclei (via absolute theoretical values of magnetic shieldings of a reference compound, see Table 2), as well as the central shielding along the C_3 axis. The construction of such a model, which should also assess the wider implication on the σ-diatropicity of C_3H_6, constitutes the essential motivation of the present paper.

2. Results and Discussion

Magnetic Properties of Cyclopropane. An extended, non-contracted (13s10p5d2f/8s4p1d) Gaussian basis set[33,45] with 435 primitives was used to optimize molecular structural parameters at the Hartree−Fock level, r_{CC} = 1.495 (5) Å and r_{CH} = 1.072 (5) Å bond distances, and HCH angle = 114.2(8)°. The same gaugeless basis set was used to evaluate near Hartree−Fock magnetizabilities, magnetic shielding of H and C nuclei, and magnetic shielding at a number of points on the $C_3 \equiv z$ symmetry axis. CO, with origin in the center of mass, and a series of CTOCD procedures were employed at the Hartree−Fock level of accuracy, that is, analytical DZ,[38,39,46] numerical DZ1[37] and PZ,[39,45,46] damped DZ2[37,47] and PZ2[39,46,47] variants. The results from different computational schemes (reported in Supporting Information) are much more accurate than those previously reported.[36] They are identical to at least three significant figures. Higher agreement among analytical and numerical methods would be obtained by increasing the accuracy of the numerical integration procedures[47] employed.

Experimental values for the magnetizability anisotropy ($\Delta\chi$) have been obtained by Aldrich et al.[13] by observing the rotational Zeeman effect with the cyclopropane−HCl and cyclopropane−HCN complexes. A definitive estimate of $\Delta\chi$ was determined by Lukins et al.[14] A value for the average magnetizability was given by Barter et al., and a slightly higher (absolute) value is quoted by Flygare.[22] The agreement between measured and theoretical properties in Table 1 is more than satisfactory in view of the fact that electron correlation effects and rotovibrational corrections should be evaluated for the latter. However, this lies beyond the scope of the present investigation.

TABLE 1: Magnetizability of Cyclopropane in 10^{29} JT^{-2}

	calc^a	exp^b	exp^c
$\chi^{d}_{\parallel}$	−243.8	−244 ± 2	
$\chi^{d}_{\perp}$	−183.3	−184 ± 2	
$\Delta\chi^{d}$	−60.5		−61.3
$\chi^{p}_{\parallel}$	161.2	168 ± 2	
$\chi^{p}_{\perp}$	119.1	125 ± 2	
$\Delta\chi^{p}$	42.1		42.0
$\chi_{\parallel}$	−82.3	−75 ± 2	−77.9 ± 1.8
$\chi_{\perp}$	−64.0	−60 ± 2	−58.7 ± 1.5
$\bar{\chi}$	−70.1	−65.1 ± 1.3^d, −66.4^e	−65.1 ± 1.3^d
$\Delta\chi$	−18.3	−15 ± 2, −17 ± 2^f	−19.2 ± 1.9

^{a}Diamagnetic and paramagnetic contributions are from the CO approach (origin in the center of mass), and average contributions are from the CTOCD-DZ approach; see text and Supporting Information. $\parallel$ and $\perp$ denote out-of-plane and in-plane components. $\Delta = \chi_{\parallel} - \chi_{\perp}$. ^{b} From Aldrich et al.[13] ^{c} From Lukins et al.[14] ^{d} From Barter et al.[21] ^{e} From Flygare.[22] ^{f} Calculated via different methods.[14]

TABLE 2: Magnetic Shielding and Chemical Shift Tensors of C and H for CH$_2$ and for the Center of Mass in Cyclopropane^a

	xx	yy	zz	av
σ^{C}	171.0	187.3	236.0	198.1
δ^{C}	23.7	7.4	−41.3	−3.4
δ^{C} exp^b	22	2	−36	−3.8
σ^{H}	33.26	26.05	36.97	32.09
δ^{H}	−1.08	6.13	−4.79	0.09
δ^{H} exp				0.22^c, 0.222^d
σ^{CM}	50.93	50.93	32.69	44.85

^{a}Values in ppm. The ^{13}C tensor is given in the principal axes system specified in the text. Coordinates: C(1.631 66, 0.0, 0.0), H(2.731 32, 0.0, −1.702 43). All shifts from tetramethylsilane. Calculated absolute values for ^{1}H and ^{13}C in TMS: σ^{H}_{av} = 32.18 ppm and σ^{C}_{av} = 194.7 ppm. ^{b} From Zilm et al.[12] ^{c} From Wiberg and Nist.[10] ^{d} From Burke and Lauterbur.[11]

Experimental values of proton chemical shift are δ^{H} = 0.22 and 0.222 ppm.[10,11] The carbon chemical shift is 196.3 ppm, referred to external CS$_2$,[11] and δ^{C} = −3.8 ppm with respect to external (CH$_3$)$_4$Si.[12] The experimental components of the chemical shift tensor reported by Zilm et al.[12] are δ^{C}_{11} = 22, δ^{C}_{22} = 2, and δ^{C}_{33} = −36 ppm, respectively.

Because the principal axes of the ^{13}C nuclear magnetic shielding are specified by the local C_{2v} symmetry, a coordinate system in which $\sigma^{C}_{11} \equiv \sigma^{C}_{xx}$, $\sigma^{C}_{22} \equiv \sigma^{C}_{yy}$, and $\sigma^{C}_{33} \equiv \sigma^{C}_{zz}$ is used in Table 2. Discrepancies found between theoretical and experimental values for the components of carbon shielding (in the liquid phase) may depend on a number of reasons that are difficult to understand. However, the average shifts of hydrogen and carbon are quite close.

The big average virtual shielding (44.9 ppm) evaluated at the center of mass (CM) corresponds to a NICS index of −44.9, according to the definition proposed by Schleyer et al.[31] (cf. with the GIAO NICS RHF/6-311+G(d,p) value of −43.0 as reported by Sauers[30] and with similar values by others).[9,27] Remarkably enough, it is mainly determined by the exceptionally large in-plane component $\sigma^{CM}_{\perp}$ = 50.9 ppm. The out-of-plane $\sigma^{CM}_{zz} \equiv \sigma^{CM}_{\parallel}$ component is $\approx$18 ppm smaller.

Because the shielding along the central z-axis is essentially biased by the electron flow in planes normal to it (see the discussion in Current Density Model in Cyclopropane), these findings are hard to reconcile with a model that assigns a dominant role to σ-ring currents. The mobile π-electrons in benzene cause an enhanced $\sigma^{CM}_{\parallel} \gg \sigma^{CM}_{\perp}$.[48] This is also the case of the cyclopropenyl cation, for which the components of

σ-Diatropicity of the Cyclopropane Molecule

J. Phys. Chem. A, Vol. 111, No. 33, 2007 **8165**

the central shielding at CM, calculated via the same basis set and DZ procedure, are $\sigma_\perp^{CM} = 27.70$ ppm and $\sigma_\parallel^{CM} = 32.47$ ppm. Therefore, if the σ-electrons sustained a strong ring current on the plane of the molecule, a similar pattern should be expected for cyclopropane. In fact, the big $\sigma_\perp^{CM}$ component for C_3H_6 is due to diamagnetic flow about the C_2 axis, as documented by the SG reported in Figure 4 of the Supporting Information.

Current Density Model in Cyclopropane. The orbital magnetic dipole moment induced in the *n* electrons of a molecule by an external magnetic field with flux density **B** is evaluated by eq 1.

$$\Delta\langle m_\alpha\rangle = \chi_{\alpha\beta}B_\beta \tag{1}$$

The magnetizability tensor ($\chi_{\alpha\beta}$) is determined by Ampère's law.

$$\chi_{\alpha\delta} = \frac{1}{2}\epsilon_{\alpha\beta\gamma}\int r_\beta \mathscr{J}_\gamma^{B_\delta}(\mathbf{r})\,\mathrm{d}^3r \tag{2}$$

The above equation introduces the current density tensor,

$$\mathscr{J}_\alpha^{B_\beta}(\mathbf{r}) = \frac{\partial}{\partial B_\beta}J_\alpha^{\mathbf{B}}(\mathbf{r}) \tag{3}$$

which is defined via the derivative of the magnetic field-induced electronic current density at **r**, $J_\alpha^{\mathbf{B}}(\mathbf{r})$. Current tensor notation is used, that is, the implicit summation rule for repeated suffixes is in force, and $\epsilon_{\alpha\beta\gamma}$ is the Levi-Civita unit tensor.[39]

The magnetic field induced at an observation point (**R**) is determined by the Biot-Savart law

$$\Delta\langle B_\alpha^n(\mathbf{R})\rangle = -\sigma_{\alpha\beta}(\mathbf{R})B_\beta \tag{4}$$

in which the shielding tensor at **R** is obtained by eq 5.

$$\sigma_{\alpha\delta}(\mathbf{R}) = -\frac{\mu_0}{4\pi}\epsilon_{\alpha\beta\gamma}\int\frac{r_\beta - R_\beta}{|\mathbf{r} - \mathbf{R}|^3}\mathscr{J}_\gamma^{B_\delta}(\mathbf{r})\,\mathrm{d}^3r \tag{5}$$

If the observation point coincides with the position $\mathbf{R}_I$ of the *I*th nucleus, carrying an intrinsic magnetic dipole $m_{I\alpha}$, then the quantity $\sigma_{\alpha\beta}(\mathbf{R}_I) \equiv \sigma_{\alpha\beta}^I$ defines the magnetic shielding tensor of that nucleus. The integrand function is interpreted as a shielding density second-rank tensor;[49,50]

$$\sum_{zz}^I(\mathbf{r}) = -\frac{\mu_0}{4\pi}\epsilon_{z\beta\gamma}\frac{r_\beta - R_{I\beta}}{|\mathbf{r} - \mathbf{R}_I|^3}\mathscr{J}_\gamma^{B_z}(\mathbf{r}) \tag{6}$$

for example, eq 6 is the *zz* component of the shielding density for nucleus *I*. This function can be plotted over a plane to analyze shielding/deshielding effects from different domains of the current density field. Because all planes perpendicular to a given direction (e.g., *z*) provide "slices" to the integral property (eq 5), one should, in principle, examine the function (eq 6) over several plot planes. In practice, only a few (from which main contributions are expected, e.g., planes of nearly maximum charge distribution) need to be sampled. According to eqs 1−5, the electronic magnetic moment $\Delta\langle m_z\rangle$ and the magnetic field $\Delta\langle B_z^n(\mathbf{R})\rangle$ induced at position **R** by an external field B_z, the magnetizability component χ_{zz}, and the nuclear shielding component $\sigma_{zz}(\mathbf{R})$ are basically determined by the components $J_x^{\mathbf{B}}$ and $J_y^{\mathbf{B}}$ of the current density flowing in the *xy* plane. The paramagnetic component $J_z^{\mathbf{B}}$ has no effect on χ_{zz} and $\sigma_{zz}(\mathbf{R})$. These statements hold for cyclic permutations of *x, y, z*.
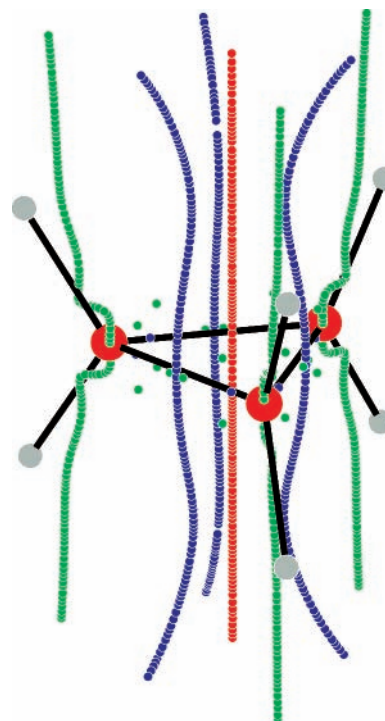

Figure 1. Perspective view of the stagnation graph of the current density vector field in cyclopropane. The uniform external magnetic field (**B** ≡ $B\epsilon_3$) is parallel to the *z*-axis. Green (red) lines denote diamagnetic (paramagnetic) vortices, and saddle lines are blue.

At a distance, the electron flow of any diamagnetic system would look like a whirlpool, also referred to as vortex, rotating anticlockwise about a north−south (NS) axis, defined by the direction of **B**. Because the electrons are negatively charged, a diamagnetic current density rotates the other way around, that is, clockwise. It vanishes along the central axis, at which the electrons stop moving.[51] Therefore, the NS axis is referred to as the primary vortical stagnation line (SL) of the *n*-electron "fluid", according to a hydrodynamical analogy. An SL is a continuous manifold of stagnation points (SP).

In the proximity of the nuclear skeleton, the external whirlpool unfolds at a branching point (BP), splitting into *m* secondary whirlpools. Each of them is associated with a vortical stagnation axis. In the boundary regions separating secondary vortices, saddle SLs are found. The branching process is regulated by the Gomes theorem,[52] according to which the number of saddle SLs emerging at a BP is *m* − 1. Phase portraits of vortical and saddle regimes are found in Figure 3 of the Gomes paper[52] and in Figure 2 of ref 39.

The set of all SLs and isolated SPs of the current density vector field constitutes its stagnation graph (SG),[52] conveying fundamental information via a compact and economical spatial model that is the embodiment of a theory of electron flow induced by magnetic fields (i.e., a simple and practical tool for assessing the magnetotropicity of a molecule). Previous investigations proved the utility of SGs for understanding the magnetic response of C_nH_n conjugated cyclic molecules[53] and heterocyclic pentatomics.[54,55] In general, an SG is a complicated topological object difficult to represent in two dimensions. Graphic software is available in the Supporting Information to observe its spatial features by rotating and magnifying the object.[56] This software is useful to understand the following discussion.

The SG in a magnetic field normal to the carbon plane of cyclopropane is shown in Figure 1. It is very different from
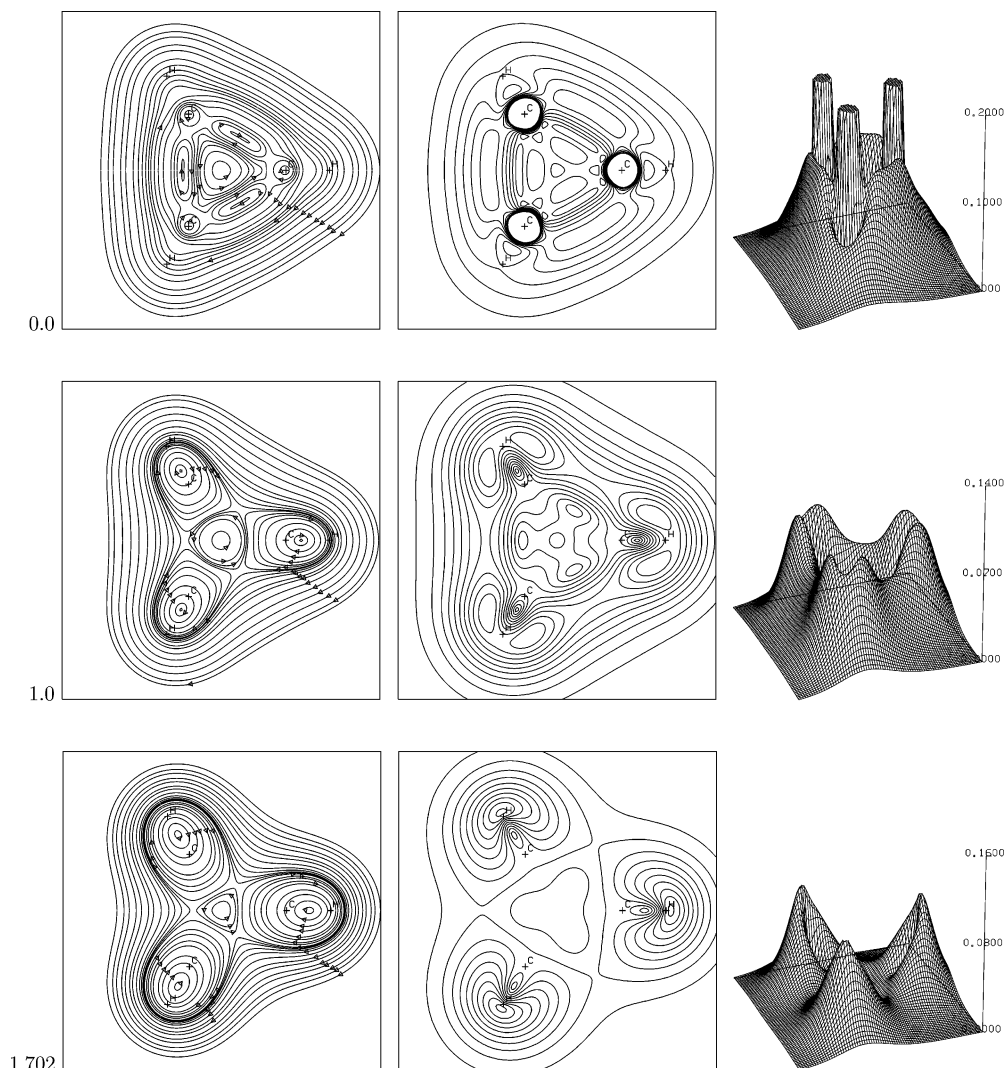
Figure 2. Streamlines and moduli of the current density vector field induced by a magnetic field (B_z) of unit magnitude normal to the xy molecular plane of cyclopropane and directed outward. The distance (in bohr) from the origin is specified by the number on the down-left corner. Atom positions are marked by crosses. The maximum moduli (step between two consecutive contours) are, in au: 2.22 (0.02) at 0.0 bohr, 0.0872 (0.009) at 1.0 bohr, and 0.0916 (0.009) at 1.702 bohr. They vary between 0.6 and 1.2 times the maximum value of the benzene π-ring current computed at the same level of theory.

that reported for aromatic C_nH_n cyclic systems, characterized by axial diamagnetic vortices originating at a BP $\approx \pm 2.5$ bohr from the σ_h plane and ending up on the C−C bonds.[53] It shows that the primary vortical SL branches out into four vortical and three saddle SLs. The BP lies on the C_3 axis, distant more than 10 bohr from the CM. Such splitting complies with the Gomes topological theorem.[52]

Three diamagnetic vortical SLs, each lying on a σ_v symmetry plane of C_3H_6, pass through the carbon nuclei, then they bend outward at some distance above and below the σ_h plane. They denote the onset of diamagnetic circulation in the sp^3 hybrid orbitals forming C−H bonds (cf. the streamline map at 1.702 bohr in Figure 2), showing that the H nuclei lie inside these diamagnetic vortices. The fourth paramagnetic vortex rotates about an SL that coincides with the C_3 axis. The streamlines in Figure 2 show the extension of the paramagnetic vortex about the center of the molecule. The corresponding contour level and three-dimensional (3D) perspective view for the intensity of the current field indicate that the central paratropic whirlpool is as weak as the diamagnetic flow in the tail regions.

The three saddle SLs, also lying on σ_v symmetry planes, cross the molecular plane slightly outside of the midpoint of the C−C bonds. The blow-up reported in Figure 7 of Supporting

Information reveals two planar diamagnetic vortices rotating at the sides of each saddle SL, close to the midpoint of a C−C bond. However, they correspond to isolated SPs, as is clearly shown by the SG in Figure 1. They do not extend in space as was found for C_nH_n conjugated cyclic molecules.[53] This pattern is entirely contained within a planar diamagnetic vortex about the center of a C−C bond. Moreover, the modulus of the local current density is ≤0.02 au, as indicated in Figure 2 by the contour showing a trough between the crosses that mark the position of carbon nuclei. (This can neatly be observed by superimposing the streamline and contour maps.) Such a trough feature indicates that delocalized ring currents about the triangular carbon framework are weak or nearly absent.

On the other hand, the 3D perspective modulus map contains a ridge, situated over the projection of an H−H direction on the σ_h plane, indicating an intensity increase in this peripheral region. Delocalized circulation takes place in the domain of the ridge just beyond the molecular perimeter. Figure 3 gives a spatial representation of the annular current density around the forked CH_2 moieties, which can be interpreted as a bona fide ring current flowing through C−C bent bonds. It is diatropic in the domains forwarding a side of the carbon triangle, but,
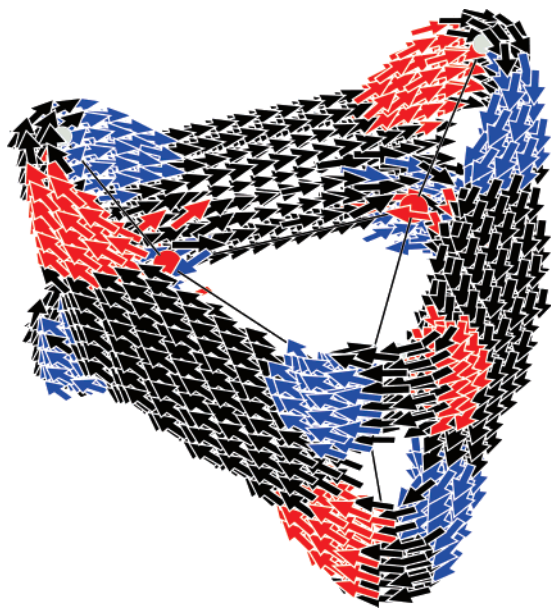
σ-Diatropicity of the Cyclopropane Molecule

J. Phys. Chem. A, Vol. 111, No. 33, 2007 **8167**

Figure 3. The ring current density flowing around the methylene groups of cyclopropane in a magnetic field normal to the molecular plane. The size of the arrows is proportional to the local modulus |$\mathbf{J^B}$|, which varies between 0.05 and 0.1 au. Red (blue) denote ascending (descending) currents. The 3D map can be rotated and magnified via the graphic code delivered in the Supporting Information.

remarkably enough, it moves up and down in the region in front of the C nuclei, which lie inside the circuit.

In the vicinity of a −CH₂ moiety, the diatropic mainstream bifurcates into two separate parts that go up and down. This feature can be compared with the "leapfrog" effect observed for π-ring currents in benzene.[57] The modulus in the ridge basin (≈0.1 au) is close to values estimated for π-ring currents in benzene.[39] A break appears in the ridge near the C nuclei (a continuous ridge is instead found for the cyclopropenyl cation; see Figure 5, Supporting Information). The regime illustrated in Figure 3 is better understood via the 3D graphic code reported in the Supporting Information by rotating and magnifying the annular electron stream in space.

Three truncated spikes of maximum modulus, orders of magnitude higher than anywhere else, are visible in the region of the carbon nuclei (see Figure 2). The enhanced value of $\chi_{\|}$ could be biased by these localized circulations to a significant extent. In fact, the local regime results from the interplay of two effects; (i) strong currents induced in the inner shell (quasiatomic 1s), which provide an isotropic contribution to the $\chi_{\alpha\beta}$ tensor; and (ii) currents flowing in the sp³ orbital along the C−H bonds (see Figures 1 and 2) above and below the molecular plane, which instead increase the magnitude of $\chi_{\|}$.

According to Ampère's law (eqs 1−2), the magnetic dipole induced by a current loop is proportional to its area. Therefore, large contributions arise from the wide region delimited by the annular circulation shown in Figure 3. However, the three diamagnetic vortices localized in the region of the C−H bonds, despite their much smaller area, are more intense than the ring current of Figure 3 near the C nuclei. From a Pascalian point of view, they account for an additive C−H bond contribution to $\chi_{\|}$. An assessment of relative weighs would be premature at the present time.

On the other hand, the model rationalizes the exceptionally high value of $\sigma_{\|}^{C}$. It is caused by the intense diamagnetic vortex with small a radius sustained by a 1s inner shell and an sp³ hybrid orbital. These vortices also provide a sizable
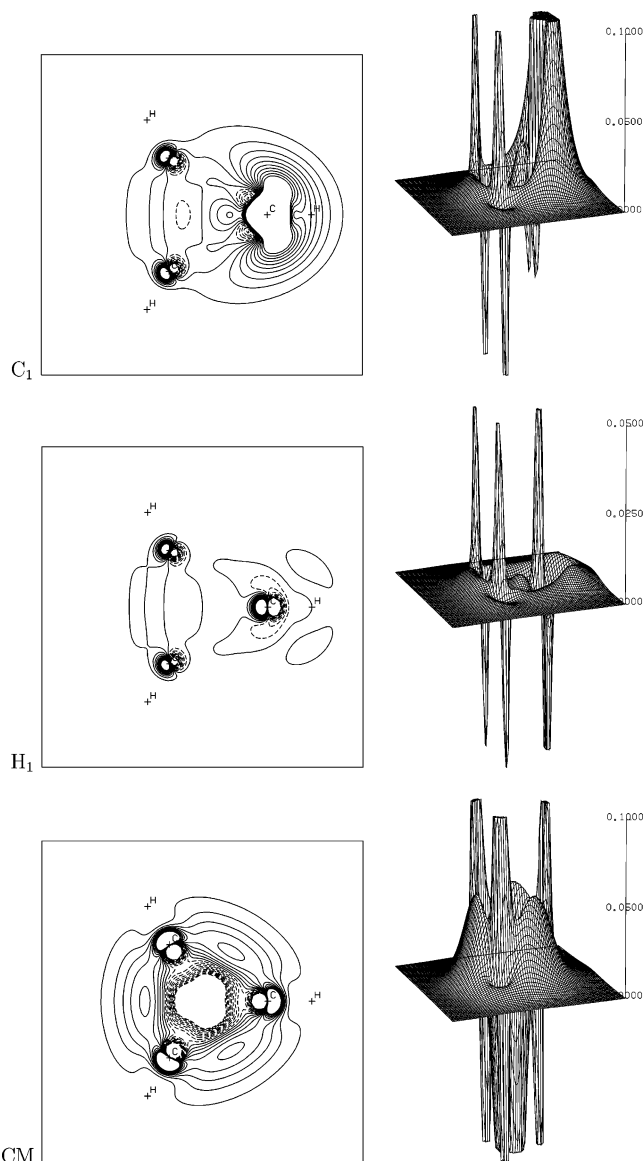

Figure 4. Magnetic shielding density (eq 6) for carbon, hydrogen, and CM on the molecular plane of cyclopropane, in au. Minimum ÷ maximum ÷ step: for C₁, −0.10 ÷ 0.10 ÷ 0.01; for H₁, −0.05 ÷ 0.05 ÷ 0.005; for CM, −0.1 ÷ 0.1 ÷ 0.01.

diamagnetic shift to σ_{zz}^{H}, as the proton lies just inside, as shown in Figure 2 (see also Figure 3, Supporting Information). Therefore, only a (minor) part of the upfield value of $\sigma_{av}^{H} = 1/3(\sigma_{xx}^{H} + \sigma_{yy}^{H} + \sigma_{zz}^{H})$ should be attributed to σ-ring currents (see the Shielding Density Maps section).

Other isolated vortex- and saddle-points are observed in the SG. Those lying on the σ_h plane match phase portraits easily recognized in the streamline maps.

Shielding Density Maps. Plots of the shielding function (eq 6) are given in Figure 4 for $I \equiv$ C, H, and CM. They account for the molecular domains where shielding/deshielding mechanisms come into operation. The effect of a current circuit on a probe is well understood.[49,50] Simple rules outlined in detail elsewhere[33−35] are used to ease interpretation of the maps. According to eq 6: (1) The sign of the shielding density ($\Sigma_{zz}(\mathbf{r})$) at point $\mathbf{r}$, contributing to shielding at position $\mathbf{R}$ of the probe, depends on the sine of the angle (θ) between the vectors $\mathbf{J^B}(\mathbf{r})$ and $\mathbf{r} - \mathbf{R}$, as their cross product appears in the Biot-Savart law. (2) $\Sigma_{zz}(\mathbf{r})$ vanishes in the vicinity of points at which $\sin\theta \rightarrow 0$ (cf. the zero contribution from ortho C atoms to the

perpendicular component of proton shielding in benzene noted by other authors).[33,35,58] (3) The out-of-plane component of the shielding of a probe inside a diamagnetic (paramagnetic) current loop goes upfield-diamagnetic shift (downfield-paramagnetic shift). (4) The shielding density diverges to $\pm\infty$ for $\mathbf{r} \rightarrow \mathbf{R}$. If $\mathbf{R}$ coincides with the center of a current loop, the current density $\mathbf{J}^B(\mathbf{R})$ vanishes. Therefore, a spike-up (spike-down) is observed about the center of a diamagnetic (paramagnetic) vortex, at which both the numerator and the denominator of eq 6 vanish.[59] (5) Contributions of opposite sign to the out-of-plane component of an external probe arise from the opposite senses of closest and furthest portions of a current loop. The typical signatures of diatropic and paratropic flow have been recognized.[33−35]

The maps of Figure 4 show sharp spikes-up (spikes-down) that denote shielding (deshielding), corresponding to continuous (dotted) contour levels localized in the region of the strong diamagnetic vortices about the remote carbon nuclei. These patterns provide nearly canceling contributions to ^{13}C. Weak net shielding from remote carbon atoms remains for ^{1}H after the negative contributions have been taken away, (cf. the different number of contours of equal step about a C nucleus). On the other hand, net deshielding arises from the nearest C.

Two distinct, peripheral continuous ridges, one passing over remote carbon atoms and the other over the cross marking the projection of the reference H nucleus on the σ_h plane, provide a hallmark of the ring currents[33−35] observed in Figure 3.

The corresponding contours extend toward the inner part, which accounts for contributions of the same magnitude from the central paratropic vortex (cf. the hill near the center of perspective map). The shielding density of eq 6 vanishes at two intermediate points, at which the vectors $\mathbf{J}^B(\mathbf{r})$ and $\mathbf{r} - \mathbf{R}_H$ become parallel and antiparallel, respectively. Analogous features are found for a number of plot planes at various distances from σ_h (e.g., for the proton shielding density on the plane of the three H nuclei in Figure 3, Supporting Information).

The map on the bottom of Figure 4 shows canceling contributions from the C-centered vortices and intense deshielding from the central paramagnetic flow. It explains why the out-of-plane component of the central shielding is much smaller than the in-plane component. However, $\sigma_{||}^{CM} = 32.7$ ppm is almost the same as the 32.5 ppm calculated for the cyclopropenyl cation via the same basis set; see the discussion in Supporting Information. The shielding that arises from the region surrounding the molecular perimeter is weak, as compared to the value ≈ 0.05 au for the ridge on a C−C bond. As shown in the maps of Figures 1 and 2 of the Supporting Information, the positive value of $\sigma_{||}^{CM}$ depends on prevailing positive contributions from higher planes along the C_3 axis.

This conclusion was checked quantitatively by calculating contributions to $\sigma_{||}^{CM}$ from various integration domains in eq 5, defined by Δz intervals along the C_3 axis. The bulk of the integral is obtained in the region $z = \pm 2.0$ bohr. Table 6 in the Supporting Information shows that the contribution from the Δz region of high σ-electron density between 0.0 and 0.2 bohr is ≈ 2 ppm, whereas that from 0.3−0.4 bohr is ≈ 2.6 ppm. The whole interval of 0.0−0.4 bohr provides ≈ 8.1 ppm, and that from 0.4 to 0.8 bohr yields ≈ 9.4 ppm.

3. Concluding Remarks

Near Hartree−Fock calculations confirm that magnetic properties of cyclopropane, for example, magnetizability and magnetic shielding at H and C nuclei, as well as experimentally accessible NMR chemical shifts from tetramethylsilane, are strongly anisotropic. Although the anisotropies $\Delta\chi$ and $\Delta\sigma^H$

could naively be explained via a model allowing for intense σ-ring currents, the large value of $\sigma_{||}^C$ eludes a description in analogous terms. The magnitude of the average shielding at the molecular CM ($\sigma_{av}^{CM} \approx 45$ppm), which is interpreted by some authors as an indicator of exceptional σ-diatropicity, is instead determined by a dominant in-plane component, $\sigma_{\perp}^{CM} \approx 51$ppm. The out-of-plane $\sigma_{||}^{CM}$ (the only component that would be biased by σ-ring currents) is ≈ 18 ppm smaller, which is also difficult to explain via the idea of enhanced σ-ring currents unless one admits that the molecule is even more σ-diatropic if the magnetic field is parallel to σ_h.

The spatial model for the current density field arrived at in the present investigation, consisting of stagnation graphs, streamline and modulus maps, and Biot−Savart shielding density maps, provides a plausible rationalization for all the components of calculated tensor properties. The anomalous upfield chemical shift of the ^{13}C nucleus is due to a strong diamagnetic vortex localized about each carbon atom and winding, to a large extent, above and below the molecular plane.

Our findings are hardly compatible with the idea of σ-ring currents of exceptional strength. In summary, the points that would seem to invalidate such hypothesis are as follows: (1) The vortices localized about the C nuclei are more intense than the currents in any other region. (2) An annular delocalized electron flow, which can be described as a σ-ring current through C−C bent bonds, was observed beyond the methylene groups. It skips the carbon nuclei, where strongly localized diamagnetic vortices are observed, and it moves up and down along the C−H bonds. The modulus of the current density field over the perimeter of the C−C−C triangle is very weak. (3) However, the intensity of the delocalized current in cyclopropane is virtually the same as that of the σ-ring currents flowing in the σ_h plane around the perimeter of conjugated C_nH_n cyclic molecules[53] and heterocyclic pentatomics.[54,55] If C_3H_6 is σ-aromatic on the magnetic criterion, then all π-aromatic C_nH_n are also σ-aromatic, which is another way of saying that none is σ-aromatic. (4) The anisotropy of the magnetizability tensor is determined by the enhanced out-of-plane component $\chi_{||}$, which could, to a significant extent, be attributed to the three intense vortices about the C−H bonds. (5) The $\sigma_{||}^H$ out-of-plane component of the hydrogen-shielding tensor is bigger than the in-plane components and dominates the average chemical shift measured in the isotropic phase. Shielding density maps show that substantial contributions to $\sigma_{||}^H$ arise from a localized diamagnetic whirlpool about the C−H bond. Less important contributions to $\sigma_{||}^H$ arise from delocalized diamagnetic ring currents and from the central paramagnetic whirlpool; see Table 8, Supporting Information. (6) Shielding density maps for the out-of-plane component of the virtual shielding at the CM of cyclopropane evidence paramagnetic shift caused by central paratropic flow. The effect of the nearby portion of localized current flowing about the C nuclei is virtually cancelled by the return current on the opposite side.

The maps show small shielding contributions from the external regions in front of C−C bonds.

Therefore, the fairly normal σ-ring current induced in cyclopropane by a magnetic field perpendicular to the molecular plane determines its peculiar magnetic properties to a minor extent. The out-of-plane components of proton and central shielding are only partially affected.

σ-Diatropicity of the Cyclopropane Molecule

J. Phys. Chem. A, Vol. 111, No. 33, 2007 **8169**

Supporting Information Available: The file contains (1) quantities used for documenting the near Hartree−Fock accuracy of calculated magnetic properties; (2) additional maps of magnetic shielding density for and for cyclopropenyl cation $C_3H_3^+$; (3) partition of magnetic shielding at the CM and proton into contributions from different spatial domains; (4) stagnation graph for in a magnetic field parallel to a $C_2 \equiv x$ symmetry axis; (5) magnification of the SG in Figure 1 in the C−C bond region; (6) LINUX and WINDOWS versions of the graphic code used to visualize 3D representations of stagnation graphs, the source for the stagnation graphs in Figure 1, for a magnetic field in the *x* direction, and for the ring currents in Figure 3. This material is available free of charge via the Internet at http://pubs.acs.org.

References and Notes

(1) Walsh, A. D. *Nature* **1947**, *159*, 712.

(2) Walsh, A. D. *Trans. Faraday Soc.* **1948**, *45*, 179.

(3) Walsh, A. D. *J. Chem. Soc.* **1953**, 2260. Consider also the series of nine following papers, pp 2266−2331 of the same issue.

(4) Coulson, C. A.; Moffitt, W. E. *J. Chem. Phys.* **1947**, *15*, 151.

(5) Coulson, C. A.; Moffitt, W. E. *Philos. Mag.* **1948**, *40*, 1.

(6) Dewar, M. J. S. *J. Am. Chem. Soc.* **1984**, *106*, 669.

(7) Cremer, D.; Kraka, E. *J. Am. Chem. Soc.* **1985**, *107*, 3800.

(8) Cremer, D.; Gauss, J. *J. Am. Chem. Soc.* **1986**, *108*, 7467.

(9) Exner, K.; von Ragué Schleyer, P. *J. Phys. Chem. A* **2001**, *105*, 3407.

(10) Wiberg, K.; Nist, B. J. *J. Am. Chem. Soc.* **1961**, *83*, 1226.

(11) Burke J. J.; Lauterbur, P. C. *J. Am. Chem. Soc.* **1964**, *86*, 1870.

(12) Zilm, K.; Beeler, A. J.; Grant, D. M.; Michl, J.; Chou, T.; Allred, E. L. *J. Am. Chem. Soc.* **1981**, *103*, 2119.

(13) Aldrich, P. D.; Kukolich, S. G.; Campbell, E. J.; Read, W. G. *J. Am. Chem. Soc.* **1983**, *105*, 5569.

(14) Lukins, P. B.; Laver, D. R.; Buckingham, A. D.; Ritchie, G. L. D. *J. Phys. Chem.* **1985**, *89*, 1309.

(15) Jackman, L. M.; Sternhell, S. *Application of Nuclear Magnetic Resonance in Organic Chemistry*, 2nd Ed; Pergamon Press: Braunschweig, 1969.

(16) Dauben, H. J.; Wilson, J. D.; Laity, J. L. In *Non-Benzenoid Aromatics*; Snyder, J. P. Ed; Academic Press: New York, 1971; Vol. 2, and references therein.

(17) Minkin, V. I.; Glukhovtsev, M. N.; Simkin, B. Y. *J. Mol. Struct.* **1988**, *181*, 93.

(18) Moran, D.; Manoharan, M.; Heine, T.; von Ragué Schleyer, P. *Org. Lett.* **2003**, *5*, 23.

(19) Pascal, P. *Compt. Rend.* **1925**, *181*, 656.

(20) Pascal, P. *Chimie Général*; Masson: Paris, 1959.

(21) Barter, C.; Meisenheimer, R. G.; Stevenson, D. P. *J. Phys. Chem.* **1960**, *64*, 1312.

(22) Flygare, W. H. *Chem. Rev.* **1974**, *74*, 653.

(23) Lacher, J. R.; Pollock, J. W.; Park, J. D. *J. Chem. Phys.* **1952**, *20*, 1047.

(24) Poulter, C. D.; Boikess, R. S.; Brauman, J. I.; Winstein, S. *J. Am. Chem. Soc.* **1972**, *94*, 2291.

(25) Hahn, R. C.; Howard, P. C. *J. Am. Chem. Soc.* **1972**, *94*, 3143.

(26) Patel, D. J.; Howden, M. H.; Roberts, J. D. *J. Am. Chem. Soc.* **1963**, *85*, 3218.

(27) Bettinger, H. F.; Pak, C. H.; Xie, Y. M.; von Ragué Schleyer, P.; Schaefer, H. F. *J. Chem. Soc. Perkin Trans.* **1999**, *2*, 2377.

(28) Jiao, H.; Nagelkerke, R.; Kurtz, H. A.; Williams, R. V.; Borden, W. T.; von Ragué Schleyer, P. *J. Am. Chem. Soc.* **1997**, *119*, 5921.

(29) Sauers, R. R.; Sonnet, P. E. *Tetrahedron* **1964**, *20*, 1029.

(30) Sauers, R. R. *Tetrahedron* **1998**, *54*, 337.

(31) von Ragué Schleyer, P.; Maerker, C.; Dransfeld, A.; Jiao, H.; van Eikema Hommes, N. J. R. *J. Am. Chem. Soc.* **1996**, *118*, 6317.

(32) Fleischer, U.; Kutzelnigg, W.; Lazzeretti, P.; Mühlenkamp, V. *J. Am. Chem. Soc.* **1994**, *116*, 5298.

(33) Ferraro, M. B.; Faglioni, F.; Ligabue, A.; Pelloni, S.; Lazzeretti, P. *Magn. Reson. Chem.* **2005**, *43*, 316.

(34) Pelloni, S.; Ligabue, A.; Lazzeretti, P. *Org. Lett.* **2004**, *6*, 4451.

(35) Soncini, A. P.; Fowler, W.; Lazzeretti, P.; Zanasi, R. *Chem. Phys. Lett.* **2005**, *401*, 164.

(36) Lazzeretti, P.; Zanasi, R. *J. Am. Chem. Soc.* **1983**, *105*, 12.

(37) Keith, T. A.; Bader, R. F. W. *Chem. Phys. Lett.* **1993**, *210*, 223.

(38) Lazzeretti, P.; Malagoli, M.; Zanasi, R. *Chem. Phys. Lett.* **1994**, *220*, 299.

(39) Lazzeretti, P. Ring Currents, In *Progress in Nuclear Magnetic Resonance Spectroscopy*; Emsley, J. W., Feeney, J., Sutcliffe, L. L. Eds; Elsevier: The Netherlands, 2000; Vol. 36, pp 1−88,

(40) Steiner, E.; Fowler, P. W. *J. Phys. Chem. A* **2001**, *105*, 9553.

(41) Soncini, A.; Fowler, P. *Chem. Phys. Lett.* **2004**, *396*, 174.

(42) Soncini, A.; Lazzeretti, P.; Zanasi, R. *Chem. Phys. Lett.* **2006**, *421*, 21.

(43) Jusélius, J. *Theoretical investigation of magnetically induced currents in closed-shell molecules, Dissertation for the degree of Doctor Philosophiae*. Department of Chemistry, University of Helsinki, 2004.

(44) Jusélius, J.; Sundholm, D.; Gauss, J. *J. Chem. Phys.* **2004**, *121*, 3952.

(45) Zanasi, R.; Lazzeretti, P.; Malagoli, M.; Piccinini, F. *J. Chem. Phys.* **1995**, *102*, 7150.

(46) Lazzeretti, P. Electric and magnetic properties of molecules, In *Handbook of Molecular Physics and Quantum Chemistry,* John Wiley & Sons, Ltd., Chichester, 2003, Vol. 3, Part 1, Chapter 3, pp 53−145.

(47) Zanasi, R. *J. Chem. Phys.* **1996**, *105*, 1460.

(48) Fallah-Bagher-Shaidaei, H.; Wannere, C. S.; Corminboeuf, C.; Puchta, R.; von Ragué Schleyer, P. *Org. Lett.* **2006**, *8*, 863.

(49) Jameson, C. J.; Buckingham, A. D. *J. Phys. Chem.* **1979**, *83*, 3366.

(50) Jameson, C. J.; Buckingham, A. D. *J. Chem. Phys.* **1980**, *73*, 5684.

(51) The average Madelung-London-Landau local velocity vanishes at stagnation points so that there is no violation of the uncertainty principle, see the discussion on p 38 of ref 39.

(52) Gomes, J. A. N. F. *Phys. Rev. A* **1983**, *28*, 559.

(53) Pelloni, S.; Faglioni, F.; Zanasi, R.; Lazzeretti, P. *Phys. Rev. A* **2006**, *74*, 012506.

(54) Pelloni, S.; Lazzeretti, P. *Theor. Chem. Acc.* **2007**, *117*, 903.

(55) Pelloni, S.; Lazzeretti, P. *Theor. Chem. Acc.* **2007**, *118*, 89.

(56) The LINUX and WINDOWS versions of the graphic code used to obtain 3D representations of the stagnation graph and current density vector field of a series of molecules can be downloaded at https://theochem.chim-far.unimo.it/VEDO3/cyclopropane.

(57) Ligabue, A.; Soncini, A.; Lazzeretti, P. *J. Am. Chem. Soc.* **2002**, *124*, 2008.

(58) Keith, T. A.; Bader, R. F. W. Can. J. Chem. **1996**, *74*, 185.

(59) For $\mathbf{r} \rightarrow \mathbf{R}$ the shielding density function behaves as $|\mathbf{r} - \mathbf{R}|^{-1}$ $(-|\mathbf{r} - \mathbf{R}|^{-1})$ for a diamagnetic (paramagnetic) vortex.